JBC RESEARCH ARTICLE

Proteomics, modeling, and fluorescence assays delineate cytochrome b_5 residues involved in binding and stimulation of cytochrome P450 17A1 17,20-lyase

Received for publication, December 17, 2023, and in revised form, January 15, 2024 Published, Papers in Press, January 26, 2024,
https://doi.org/10.1016/j.jbc.2024.105688

Yasuhiro Tateishi[1], Stephany N. Webb[1], Bian Li[2], Lu Liu[1], Kristie Lindsey Rose[1,3], Micheal Leser[3], Purvi Patel[3], and F. Peter Guengerich[1,*]

From the [1]Department of Biochemistry, Vanderbilt University School of Medicine, Nashville, Tennessee, USA; [2]Department of Medicine, Vanderbilt University Medical Center, Nashville, Tennessee, USA; [3]Proteomics Laboratory, Mass Spectrometry Research Center, Vanderbilt University School of Medicine, Nashville, Tennessee, USA

Reviewed by members of the JBC Editorial Board. Edited by Joseph Jez

Cytochrome b_5 (b_5) is known to stimulate some catalytic activities of cytochrome P450 (P450, CYP) enzymes, although mechanisms still need to be defined. The reactions most strongly enhanced by b_5 are the 17,20-lyase reactions of P450 17A1 involved in steroid biosynthesis. We had previously used a fluorescently labeled human b_5 variant (Alexa 488-T70C-b_5) to characterize human P450 17A1-b_5 interactions, but subsequent proteomic analyses indicated that lysines in b_5 were also modified with Alexa 488 maleimide in addition to Cys-70, due to disulfide dimerization of the T70C mutant. A series of b_5 variants were constructed with Cys replacements for the identified lysine residues and labeled with the dye. Fluorescence attenuation and the function of b_5 in the steroid lyase reaction depended on the modified position. Apo-b_5 (devoid of heme group) studies revealed the lack of involvement of the b_5 heme in the fluorescence attenuation. A structural model of b_5 with P450 17A1 was predicted using AlphaFold-Multimer algorithms/Rosetta docking, based upon the individual structures, which predicted several new contacts not previously reported, that is, interactions of b_5 Glu-48:17A1 Arg-347, b_5 Glu-49:17A1 Arg-449, b_5 Asp-65:17A1 Arg-126, b_5 Asp-65:17A1 Arg-125, and b_5 Glu-61:17A1 Lys-91. Fluorescence polarization assays with two modified b_5 variants yielded K_d values (for b_5-P450 17A1) of 120 to 380 nM, the best estimate of binding affinity. We conclude that both monomeric and dimeric b_5 can bind to P450 17A1 and stimulate activity. Results with the mutants indicate that several Lys residues in b_5 are sensitive to the interaction with P450 17A1, including Lys-88 and Lys-91.

Cytochrome b_5 (b_5, CYB5A) is a small (~18 kDa) accessory protein involved in several reactions, including fatty acid desaturation. It is involved in several cytochrome P450 (P450, CYP)-catalyzed reactions, including xenobiotic metabolism, fatty acid metabolism, and steroid biosynthesis, either inhibiting or stimulating. In some cases there is evidence that b_5 transfers the second electron (received from NADPH-cytochrome P450 reductase (POR) or NADH-cytochrome b_5 reductase) to the $Fe^{2+}O_2$ complex of P450 (1, 2), but in many cases b_5 is believed to act as an allosteric partner, modulating the conformation of P450s upon binding (3–5). However, a definitive mechanism of this function remains unclear in the absence of binary crystal structures.

One of the enzymes whose catalytic activity is strongly enhanced by b_5 is P450 17A1, also known as steroid 17α-hydroxylase/17,20-lyase. The enzyme is localized in steroidogenic tissues (e.g., adrenal glands, testis, and ovaries) and mainly catalyzes 2-step oxidations of steroids, namely 17α-hydroxylation and the subsequent 17,20 C-C bond cleavage (the so called "lyase" reaction), to yield androstenedione and dehydroepiandrostenedione (Fig. 1). Although these two reactions are the major ones involved with progesterone and pregnenolone, some minor pathways (*e.g.*, 16α-hydroxylation) are also known (6). P450 17A1 plays an essential role in producing androgens as well as 17α-hydroxy steroids, which are further converted to mineralocorticoids and glucocorticoids. The enzyme is involved in some human maladies, including breast cancer (7), polycystic ovary syndrome (8, 9), Cushing's syndrome (10), glioblastoma (11), and particularly prostate cancer (12). Although numerous efforts have been devoted to developing P450 17A1 inhibitors, only one drug, abiraterone (prodrug abiraterone acetate), has been approved for the treatment of castration–resistant prostate cancer. However, this drug is known to have major side effects because of its nonspecific inhibition of other P450 enzymes (13–15) and nonselectivity between the 17α-hydroxylation and 17,20-lyase reactions of P450 17A1 (Fig. 1) (12, 16). Therefore, the discovery of more selective lyase inhibitors (which would only reduce the production of androgens) is still desired. The b_5-P450 17A1 interaction is of great interest from both clinical and biochemical viewpoints because b_5 has been shown to play an essential role in 17,20-lyase reactions catalyzed by P450 17A1 but has little or no effect on 17α-hydroxylations (17–19).

* For correspondence: F. Peter Guengerich, f.guengerich@vanderbilt.edu.
Present addresses for: Stephany N. Webb, Center for Pharmacogenetics, Department of Pharmaceutical Sciences, University of Pittsburgh School of Pharmacy, Pittsburgh, Pennsylvania, USA; Bin Li, Regeneron Pharmaceuticals Inc, Tarrytown, New York, USA; Lu Liu, University of Illinois at Urbana-Champaign, Urbana, Illinois, USA.

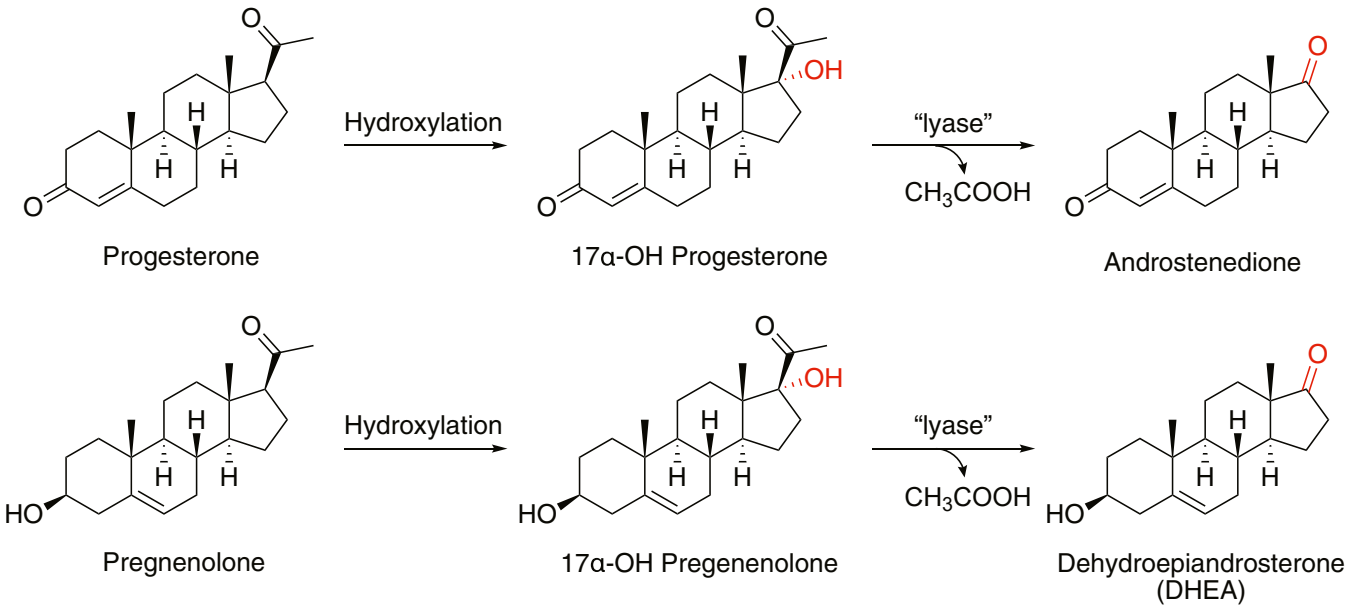

Figure 1. Major reactions catalyzed by P450 17A1.

Structures of both human b_5 and P450 17A1 (20) are available, but to our knowledge no crystal structure of a b_5-P450 17A1 protein complex has been reported. Nevertheless, many studies have been published on the functions of this interaction. It is generally accepted that b_5 allosterically stimulates lyase reactions by inducing conformational changes of P450 17A1, not by electron transfer from b_5 to P450 17A1 (4, 21, 22). More than 125 clinical variants of P450 17A1 have been reported (20), and some of these (e.g., R347C, R347H, R347Q, R358Q, P428L, F417C, and E305G) are known to preferentially affect the lyase activity *in vivo* (23–25). The variants R347H, R347Q, and R358Q are considered to be deficient due to the loss of ability to bind to b_5 (23, 26, 27). Similarly, the Glu-48 and Glu-49 residues of b_5 are critical for the lyase activity (28) and clinical variants are known with serious endocrinological issues (29, 30). The importance of these residues is further supported by experimental data utilizing site-directed mutagenesis, NMR spectroscopy, and chemical crosslinking, indicating that ionic interactions between acidic residues of b_5 and basic residues of P450 17A1 are critical (28, 31, 32).

One of the issues in the field is that there are few useful assays for the analysis of the interactions between b_5 and P450 enzymes. Surface plasmon resonance-based assays have been used with b_5 and P450 17A1, with a reported K_d value of 440 nM (33). However, this approach has caveats due to the need to immobilize one protein and a major deficiency is "mass transfer," a term used to describe the diffusion of the ligand from the solution through the matrix to reach the receptor (P450 17A1) (34). NMR spectroscopy has also been used to investigate this interaction qualitatively (35), but this approach has issues in estimating the low K_d value because high concentrations of the proteins are required. Simonov *et al.* (21) reported FRET-based assays that used fluorescent protein-fused P450 17A1 and b_5 to successfully demonstrate the interaction within cells. We have used a fluorescently labeled b_5 T70C variant, observing the fluorescence attenuation by titrating with P450 enzymes (19, 36).

To better understand b_5-P450 17A1 interactions, we further investigated fluorescence-based protein-protein interaction assays. Site-directed mutagenesis was conducted to construct a series of Lys-to-Cys b_5 variants for selective labeling, based on the lysine residues modified with Alexa Fluor 488 maleimide. A structure for b_5-P450 17A1 complex was modeled via AlphaFold-Multimer (AFM) protein complex structure prediction (37) and Rosetta protein-protein docking (38). The modeled structure agrees well with existing knowledge about b_5-P450 17A1 interaction and also suggests potential new interactions for further experimental investigation. The fluorescence attenuation of Alexa 488-conjugated b_5 mutants (by P450 17A1) varied depending on the labeled position. A fluorescence polarization assay was also developed to study the binding, and the K_d value of the binding was estimated in the sub-μM range (130 nM under these conditions).

Results

Preparation of Alexa 488-labeled WT human b_5 *and titration with P450 17A1*

In previous work, we labeled a human b_5 mutant (T70C) with a green fluorophore (Alexa Fluor 488 C5 maleimide) and used it to characterize the interaction between b_5 and human P450s (19, 36). In the course of further studies with Alexa 488-labeled T70C b_5 (Alexa 488-T70C-b_5), we found that this protein exists mainly as a dimer that was disrupted by thiols (e.g., high concentrations of DTT), implying that the thiol in the cysteine residue was forming a disulfide bond instead of reacting with the maleimide group of Alexa 488 dye (Fig. 2). The requirement for a high concentration of DTT (10 mM, Fig. S1) was surprising in light of our finding of near-maximal

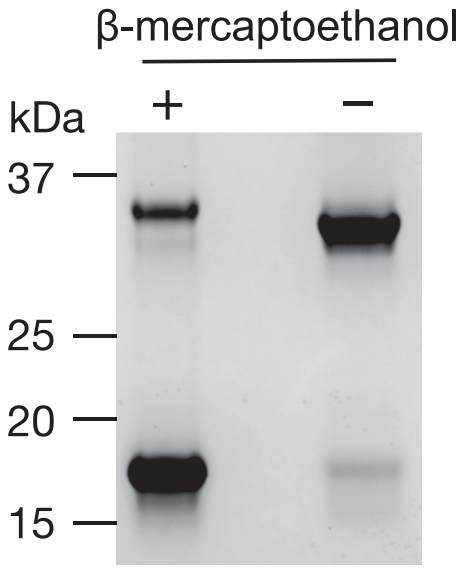

Figure 2. SDS-PAGE of previously construct of Alexa 488-T70C-b_5 (19). Proteins were separated on a 10% Bis-tris polyacrylamide gel with MES running buffer. Alexa 488-T70C-b_5 (200 pmol) was loaded either with (*left lane*) or without (*right lane*) pretreatment with β-mercaptoethanol (10%, v/v). The gel was imaged by total protein staining by SimplyBlue Safe Stain (Thermo Fisher Scientific). The monomer migrated at 17 kDa and the dimer at 34 kDa, with some difference in mobility of the dimer in the sample containing β-mercaptoethanol. MES, 2-[*N*-morpholino]ethanesulfonic acid.

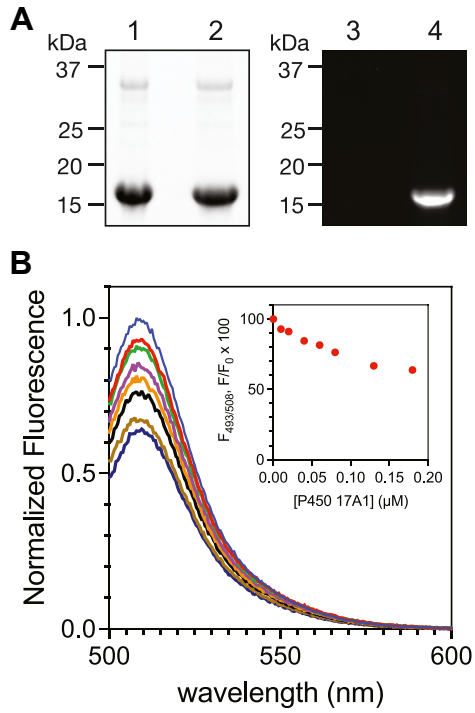

Figure 3. Construction of Alexa 488-WT-b_5 and fluorescence titration with P450 17A1. *A*, SDS-PAGE of nonlabeled (lanes 1, 3) or Alexa 488-labeled WT b_5 (lanes 2 and 4). The gel was imaged by total protein staining by SimplyBlue Safe Stain (Thermo Fisher Scientific) (lanes 1 and 2) or excited with 493 nm light (lanes 3 and 4); *B*, a solution of Alexa 488-WT b_5 (50 nM) was excited at 493 nm in a spectroflourimeter and the attenuated emission spectra (500–600 nm) were recorded following addition of increasing concentrations of P450 17A1. The emission spectra were normalized to the initial (maximum) fluorescence intensity. The inset shows the normalized fluorescence data points at the emission wavelength maximum (508 nm) in fluorescence titrations.

stimulation of the laurate ω-hydroxylation activity of P450 4A11 by 50 μM DTT or tris(2-carboxyethyl)phosphine (39). We also found that tris(2-carboxyethyl)phosphine was not effective in reducing the disulfide linkage of the b_5 dimer (Fig. S1). (In a previous study with rat b_5 and bacterial P450 101A1, Stayton *et al.* (40) had used 10 mM DTT to reduce the corresponding (rat b_5) T65C mutant prior to modification with another reagent but did not comment on the need for use of a high concentration to prevent dimerization.)

Based on this observation, monomeric Alexa 488-labeled WT b_5 (Alexa 488-WT-b_5, devoid of Cys residues) was prepared by reaction with the fluorophore overnight at room temperature, using the same conditions as previously mentioned (19) (Fig. 3*A*). The product was desalted and titrated with P450 17A1 in 1 mM potassium phosphate buffer. The fluorescence intensity was attenuated by the addition of P450 17A1 (Fig. 3*B*), as observed previously in the case of Alexa 488-T70C-b_5 (19). Only minimal inner-filter effects (∼3%) were observed within the range of P450 17A1 concentrations we examined (Fig. S2). The addition of WT b_5 eliminated the attenuation of fluorescence intensity, providing evidence that the observed fluorescence attenuation was due to the binding of the modified b_5 to P450 17A1 (Fig. S3, *A* and *B*). Titration in buffer with higher ionic strength (100 mM potassium phosphate) resulted in less attenuation of fluorescence (Fig. S3, *C* and *D*), consistent with previous reports that the interaction between b_5 and P450 17A1 involves ionic interactions (31, 32).

Mechanistic study of fluorescence attenuation using apo-b_5

The absorbance spectra of P450 17A1 and b_5 showed considerable overlap with the absorbance (excitation) spectrum of the Alexa-488 fluorophore (Fig. 4*A*), suggesting the possibility that the heme in one or both enzymes is related to the observed fluorescence attenuation. Accordingly, the apo form of b_5 (apo-b_5) was prepared by treating WT b_5 (holo form) with acid in acetone (3, 41) to remove the heme. Apo-b_5 was modified with Alexa 488 to prepare Alexa 488-apo-b_5 (using the same procedure used to prepare Alexa 488-WT-b_5) and then titrated with hemin or P450 17A1. The fluorescence of both Alexa-modified apo- and holo-b_5 was attenuated to a similar extent (Figs. 3*B*, and 4, *B* and *C*). When titrated with hemin, the fluorescence of Alexa 488-apo-b_5 was attenuated although Alexa 488-WT b_5 (holo-form) showed little quenching upon titration (Fig. 4, *D*–*F*). No change in the fluorescence spectra of free Alexa 488 C5 maleimide dye was observed following the addition of either hemin or P450 17A1 (Fig. S4). Collectively these results are interpreted to mean that the observed attenuation of Alexa 488-b_5 fluorescence was not due to the b_5 heme prosthetic group, but the attenuation of fluorescence can be due to either the protein P450 17A1 or possibly its heme group.

Proteomic analysis of sites of Alexa 488 labeling in modified b_5

In light of the results demonstrating the covalent binding of Alexa 488 to b_5 dimer (Fig. 2), in which the only Cys residue in the T70C mutant b_5 was tied up in a disulfide linkage, we

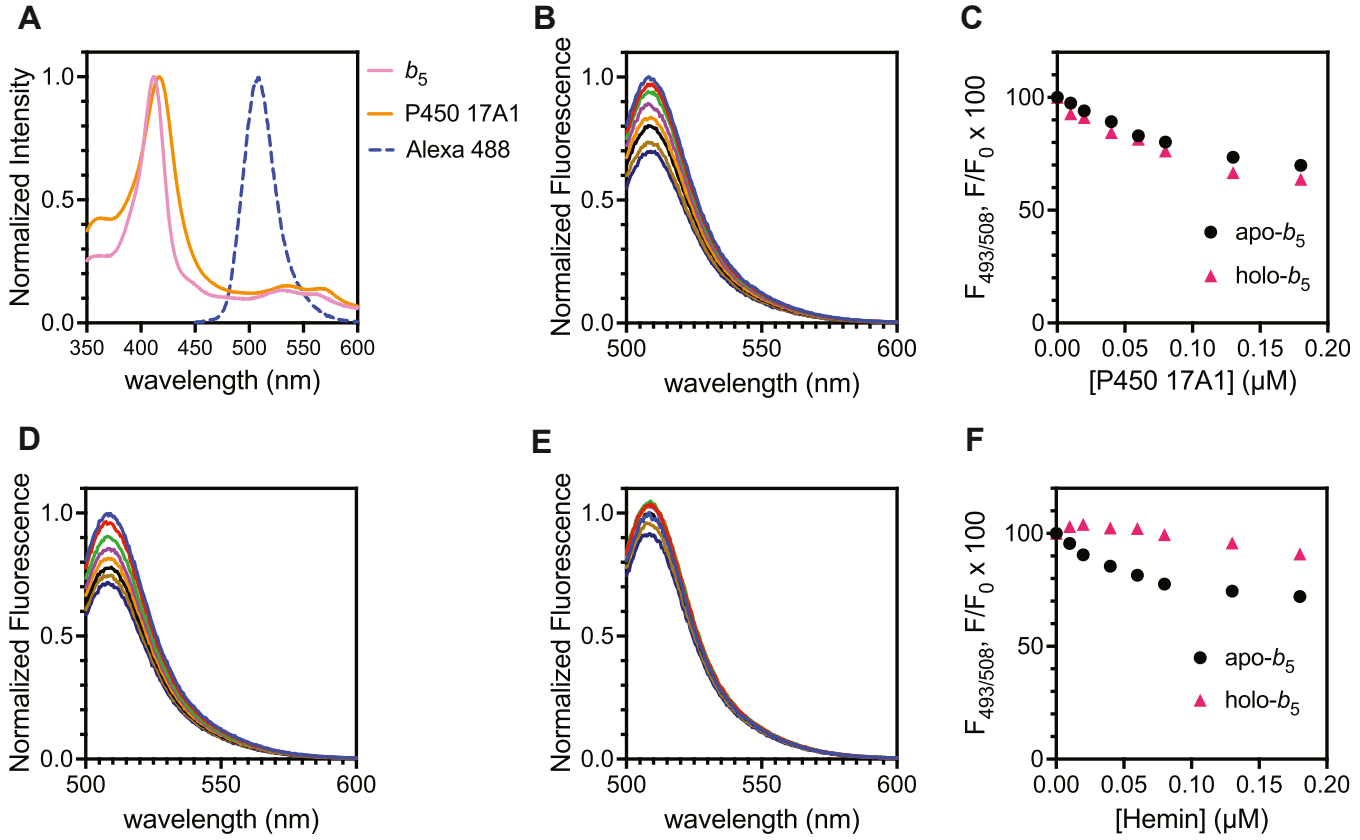

Figure 4. Effect of heme in b_5 on fluorescence titration. *A*, normalized absorbance spectra (*solid line*) of b_5 (*pink*) or P450 17A1 (*orange*) and fluorescence (emission) spectra of Alexa 488 (*stippled line, blue*); *B*, representative normalized fluorescence spectra of Alexa 488-apo-b_5 (50 nM) with increasing concentrations of P450 17A1; *C*, F/F_0 plot of the normalized fluorescence when titrated with P450 17A1. (The data with holo-b_5 (Alexa 488-WT b_5) were the same as in the experiment of Fig. 3*B*); *D* and *E*, representative normalized fluorescence spectra of Alexa 488-apo-b_5 (*D*) and Alexa 488-WT b_5 (*E*) with increasing concentrations of hemin; *F*, F/F_0 plot of the normalized fluorescence when titrated with hemin.

hypothesized that lysine residues in WT b_5 reacted with the maleimide group of Alexa 488, based on established literature precedent (42). Accordingly, the fluorescence attenuation in titrations with P450 17A1 would be linked with alterations in the environments of these residues. To determine which amino acids had reacted with the Alexa 488 fluorophore, proteomic analysis of Alexa 488-WT-b_5 was conducted. Following SDS gel electrophoresis, b_5 was digested with trypsin and the resulting peptides were analyzed by high-resolution mass spectrometry (Table S1). The data indicated that six of the eight lysines (Lys-10, Lys-19, Lys-24, Lys-33, Lys-39, and Lys-77), as well as the *N*-terminal amino group in WT b_5, were labeled with the Alexa fluorophore (tandem mass spectra of each modified peptide are shown in Fig. S5, and a list of detected peptides is shown in Table S2).

Computational modeling of the structure of b_5-P450 17A1 complex

A 3-dimensional structural model of P450 17A1 bound to b_5 was built by combining deep-learning based multimeric protein structure prediction and biophysics-based modeling and docking (see Experimental Procedures). Briefly, AFM algorithms (37) were used to generate a starting model of a b_5-P450 17A1 complex. This model was then energy-minimized and used to perform protein-protein docking to further sample the binding poses between b_5 and P450 17A1 using the Rosetta modeling suite (38). The model revealed that Arg-347 and Arg-358 in P450 17A1 are close to Glu-48 and Glu-49 in b_5, as reported in chemical crosslinking studies by Peng *et al.* (32) and other lines of investigation (23, 24, 28, 31), providing confidence about the results of the final model (Fig. 5*A*, Tables 1, and 2). Among the Alexa 488-labeled amino residues that we identified in b_5 (see above), the *N*-terminus and Lys-10 are located relatively far away from the heme prosthetic groups in P450 17A1 and from the putative site of interaction (Fig. 5*B*). Thus, we focused on the other five positions, that is, Lys-19, Lys-24, Lys-33, Lys-39, and Lys-77 in the following investigations.

Preparation of Alexa 488-labeled human b_5 mutants and titration with P450 17A1

To modify single amino acid residues in b_5, a series of mutant b_5 proteins with cysteine substituted for individual lysines (K19C, K24C, K33C, K39C, and K77C) was constructed (Table S3). Gel electrophoresis in the absence and presence of β-mercaptoethanol showed that the T70C and K24C mutants existed largely as disulfide dimers. All of the mutant b_5 enzymes were treated with 10 mM DTT (see above) prior to labeling with Alexa 488 C5 maleimide to prevent formation of disulfide-linked dimers and then reacted with a 5-fold

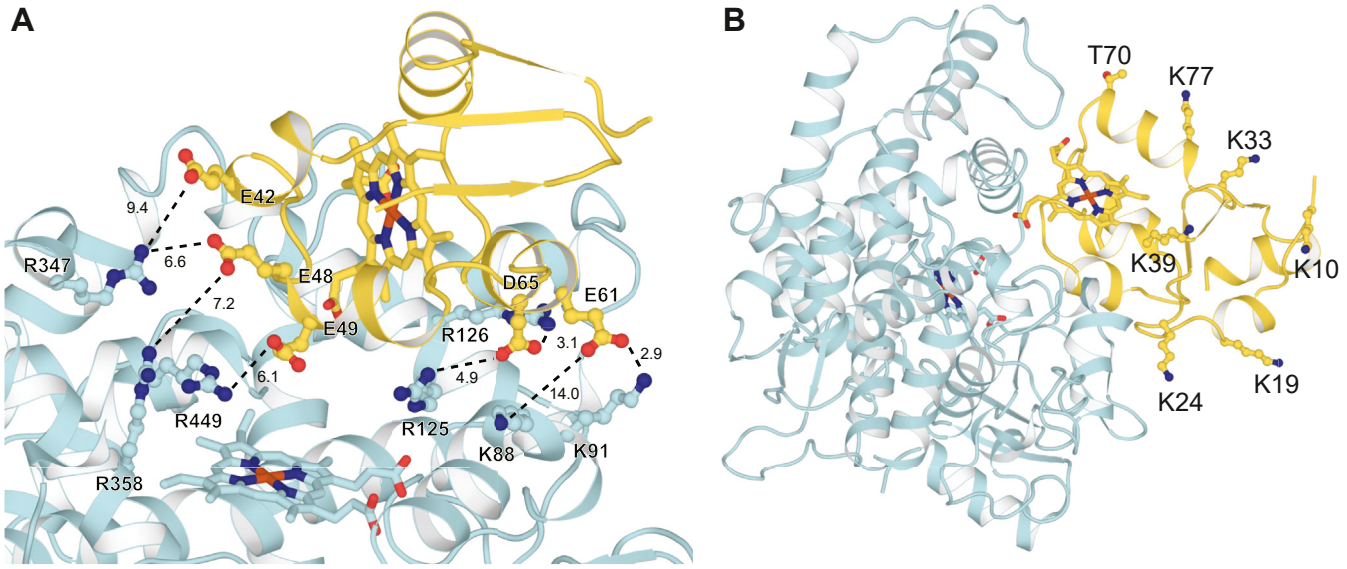

Figure 5. AlphaFold-Multimer-derived models of b_5:P450 17A1 binary complex. *A*, the two negatively charged patches in b_5 (*yellow*), *i.e.* E42, E48, E49 and E61, D65 are in close proximity with positively charged patches in P450 17A1 (*cyan*), *i.e.* R347, R358, R449 and K91, R125, R126. Interestingly, the P450 17A1 residue K88, which was reported by Peng *et al.* (32) to interact with E61 in b_5, is relatively far away from E61 in our model. Given the long sidechain of K88, it is likely that K88 can interact with E61 after adopting a different side-chain rotamer. Numbers next to *dashed lines* represents the distances (in Å) between the corresponding pair of atoms. *B*, locations of b_5 residues K10, K19, K24, K33, K39, T70, and K77. Their distances to the b_5-heme and P450 17A1-heme are tabulated in Table 1.

molecular excess of Alexa 488 C5 maleimide at room temperature for 2 h, conditions designed for selective modification of the single Cys in each protein. Pretreatment with the reducing reagent DTT yielded essentially quantitative reduction of any linked dimers (as judged by gel analysis), which were then reacted with a 5-fold molecular excess of Alexa 488 C5 maleimide at room temperature. The labeling efficiency was nearly quantitative, based on the calculations with the absorbance spectra, and the presence of only a single labeled b_5 peptide at the mutated Cys was confirmed by the proteomic analysis (Fig. 6, Tables S1, and S2, showing T70C b_5 data).

Titration of all the Alexa 488-modified mutant b_5 proteins and P450 17A1 showed some loss of fluorescence intensity, as observed in Alexa 488-WT b_5 (Fig. 3*B*), but the character of the saturation curves depended on the site of labeling (Fig. 7). Alexa 488-WT, -T70C, and -K77C-b_5 showed the greatest attenuation (Figs. 3*B*, and 7, *E* and *F*), Alexa 488-K24C and -K39C-b_5 showed moderate changes (Fig. 7*B*, 7*D*), and Alexa 488-K19C and -K33C-b_5 had little change upon titration (Fig. 7, *A* and *C*). Interestingly, Alexa 488-T70C and -K77C-b_5 showed slightly enhanced fluorescence intensity with the addition of a very low concentration of P450 17A1 (~8% increase), followed by attenuation up to and beyond a stoichiometric concentration (Fig. 7, *E* and *F*). The attenuation of fluorescence intensity caused by the binding of P450 17A1 to these modified b_5 proteins could also be eliminated by the addition of unlabeled WT b_5 (Fig. S6), indicating that the observed fluorescence attenuation of labeled b_5 was due to the binding to P450 17A1.

The K19C mutant, which did not show very much fluorescence attenuation after labeling (Fig. 7*A*), was examined further. SDS-PAGE indicted that the M_r of this protein was ~3 kDa lower than that of WT b_5 or the other mutants (Fig. S7), and accordingly it was not used in further analyses (the basis of the lower M_r was not analyzed).

Catalytic activity of P450 17A1 enhanced by unmodified or modified b_5 proteins

It is well-established that human and other P450 17A1 enzymes require b_5 for the steroid 17,20-lyase reaction (17, 19, 43, 44). To examine if the Alexa 488 labeling of b_5 causes the loss of P450 17A1 activity, the lyase activity was measured using our previously reported LC-MS procedure (16, 45)

Table 1
Distances (in Å) between heteroatoms in side chains of some b_5 residues and the P450 17A1 heme iron atom

Residue	Atom	Distance, Å
Lys-10	Nζ	40.1
Lys-19	Nζ	36.9
Lys-24	Nζ	29.8
Lys-33	Nζ	36.2
Lys-39	Nζ	32.6
Thr-70	O	28.9
Lys-77	Nζ	33.3

Table 2
Distances (in Å) between b_5 oxygen and P450 17A1 nitrogen atoms of interacting residues identified by modeling (Fig. 5*A*)

b_5 residue	P450 17A1 residue	Distance, Å	Previous report
Glu-42	Arg-347	9.4	(32)
Glu-48	Arg-347	6.6	
Glu-48	Arg-358	7.2	(32)
Glu-49	Arg-449	6.1	
Asp-65	Arg-126	3.1	
Asp-65	Arg-125	4.9	
Glu-61	Lys-88	14.0	(32)
Glu-61	Lys-91	2.9	

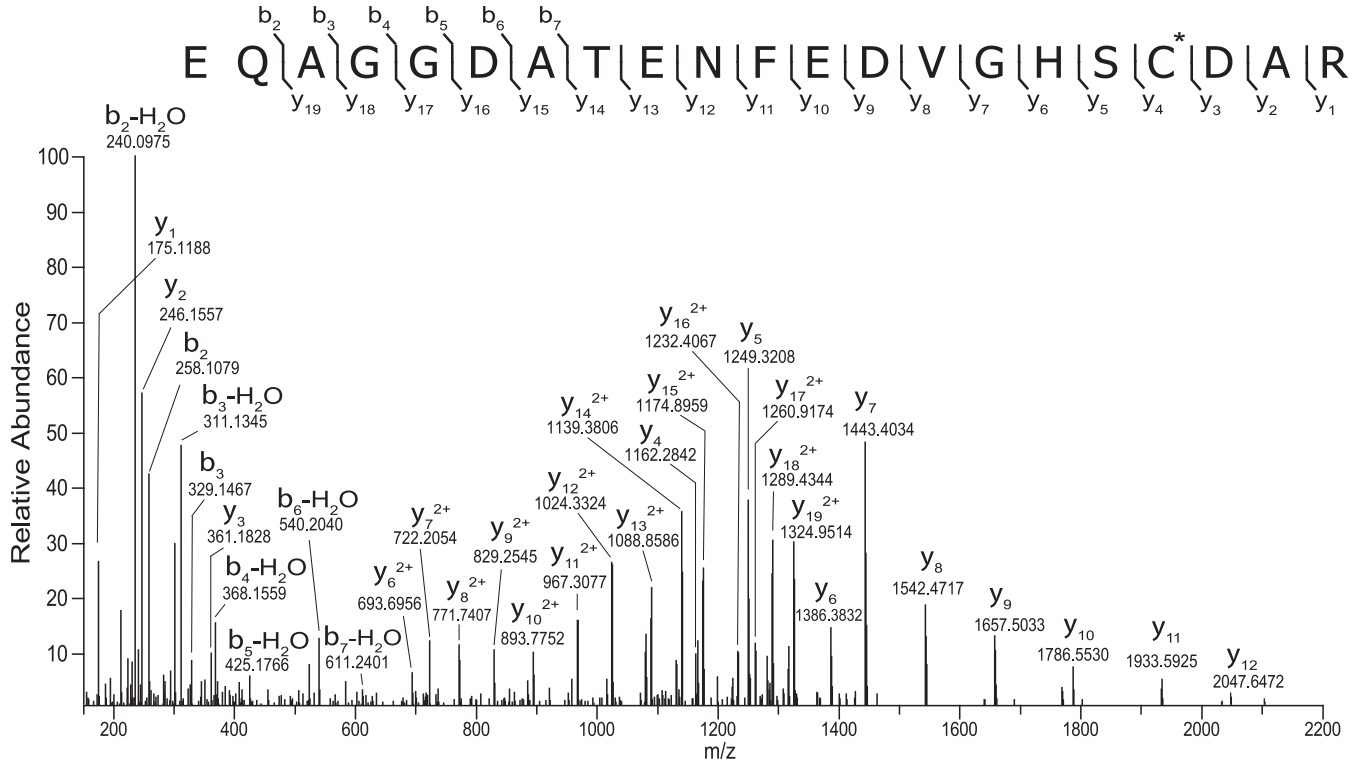

Figure 6. Tandem mass spectrum of peptide, EQAGGDATENFEDVGHSCDAR, modified at C70 with the Alexa488. The $[M+3H]^{3+}$ precursor ion was selected for fragmentation, and the observed b- and y-type product ions are assigned to their corresponding *m/z* peaks in the mass spectrum. The amino acid sequence is provided above the annotated spectrum with the position of the Alexa 488 fluorophore (+698.0989) modification denoted by the asterisk (*), and sites of amide bond fragmentation are indicated with interresidue brackets.

(Fig. 8). With most of the mutant b_5 proteins, except for K24C, lyase rates were only somewhat lower compared to WT b_5. Lyase activity was below the limit of detection without the addition of b_5, as described previously (16, 19, 45).

We measured the rates of electron transfer from NADPH to POR to WT b_5 and each of the b_5 mutants (Fig. S8 and Tables S4). Reduction of WT b_5 was rapid, as expected (46). Rates of electron transfer were compromised for all the mutants, and these rates did not bear a relationship to the stimulation of lyase activity. This result is not surprising, in the light of evidence against a requirement for electron transfer to or from b_5 in stimulation (2, 4, 22, 47). However, even the lowest rates (*e.g.*, with K70C-b_5, Table S4) were faster than the lyase reaction, so they may not be incompatible with a role of ferrous b_5. The roles of the individual lysine residues (and Thr-70) in electron transfer and (most likely) in binding of POR and b_5 are unknown and, to our knowledge, have not been examined by others.

The Alexa 488 probe did not impair the function of b_5 very much in most cases, and with K33C-b_5 and T70C-b_5, the enzyme activity was somewhat enhanced by fluorescent labeling (note that the Eyring-Polanyi equation equates a 2-fold rate change with <0.5 kcal mol^{-1} change in free energy (48), thus small differences only reflect very modest changes in the free energy of binding parameters). We conclude that the fluorescence changes observed with labeled b_5 proteins are indicative of productive interactions with P450 17A1.

Fluorescence polarization assays of binding of b_5 to P450 17A1

Fluorescence polarization is a widely accepted method for the study of protein-protein, protein-peptide, and protein-nucleic acid interactions (49). The photochemical properties of Alexa 488 dye are known to be applicable to fluorescence polarization methods, and accordingly Alexa 488 labeled b_5 was used to develop a fluorescence polarization assay with P450 17A1. The Alexa 488-T70C and -K77C-b_5 proteins showed the most fluorescence attenuation in the P450 17A1 titrations (Fig. 7). A preliminary study suggested that these two modified proteins showed a greater dynamic range compared with other modified b_5 mutants (data not presented), and the calculated K_d values were 379 and 125 nM, respectively (Fig. 9, *A* and *B* and Table 3). Increasing the ionic strength of the binding buffer was unfavorable for detection of fluorescence polarization (Fig. S9), consistent with previous reports on b_5:P450 17A1 interactions (31, 32). Alexa 488-K77C-b_5 also showed fluorescence polarization with other P450 enzymes in a concentration-dependent manner (Fig. S10), suggesting the general applicability of the fluorescence polarization-based assay for the study of b_5-P450 interactions.

In fluorescence polarization work, it is common to label low M_r peptides with fluorescent probes. In our previous study, a peptide consisting of the putative b_5 binding site of P450 17A1 (residues 348–358, "P450 17A1 peptide") showed weak inhibitory activity against the lyase reaction in a reconstituted system (19). This P450 17A1 peptide was added to an Alexa

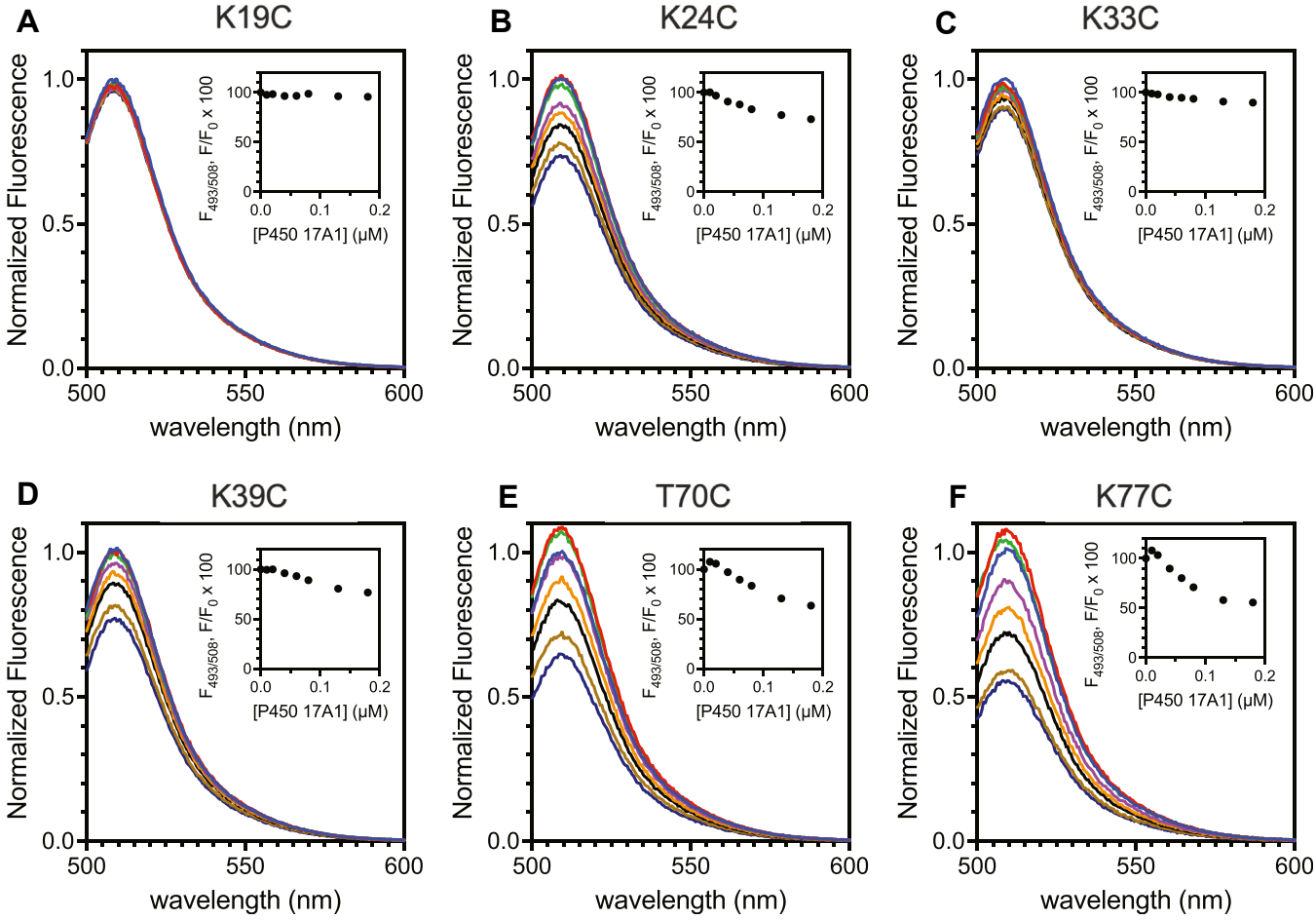

Figure 7. Fluorescence titration of Alexa 488-mutant b_5s with P450 17A1. Titrations were performed in 1 mM potassium phosphate buffer (pH 7.4) with Alexa 488-labeled human b_5 variants (50 nM) and P450 17A1 (0, 0.01, 0.02, 0.04, 0.06, 0.08, 0.13, and 0.18 μM). The emission spectra were normalized to maximum fluorescence intensity of each Alexa 488-labeled b_5 mutant. The insets show the normalized fluorescence data points at the emission wavelength maximum (508 nm) in fluorescence titrations. *A*, Alexa 488-K19C-b_5; *B*, Alexa 488-K24C-b_5; *C*, Alexa 488-K33C-b_5; *D*, Alexa 488-K39C-b_5; *E*, Alexa 488-T70C-b_5; and *F*, Alexa 488-K77C-b_5.

488-labeled b_5:P450 17A1 complex, with the expectation that the peptide would disrupt the polarization in a concentration-dependent manner. However, the peptide increased the polarization instead of decreasing it, indicating that the P450 17A1 peptide was binding to b_5 (results not shown). Accordingly, fluorescence polarization assays with the P450 17A1 peptide were conducted using Alexa 488-T70C and -K77C-b_5 (Fig. 10, *A* and *B*). The P450 17A1 peptide produced fluorescence polarization (Fig. 10, *A* and *B*; K_d values 113 and 52 μM, respectively), although the affinity was weak. This binding was disrupted by the addition of nonlabeled WT b_5 (Fig. 10, *C* and *D*). On the basis of these results, we prepared an Alexa 488-labeled P450 17A1 peptide, which had the modification at either the *N* or *C* terminus. However, no fluorescence polarization was observed when the Alexa 488-labeled P450 17A1 peptide was incubated with concentrations of WT b_5 up to 10 μM, indicating that these modified peptides did not bind to b_5 (Fig. S11), at least not generating a signal.

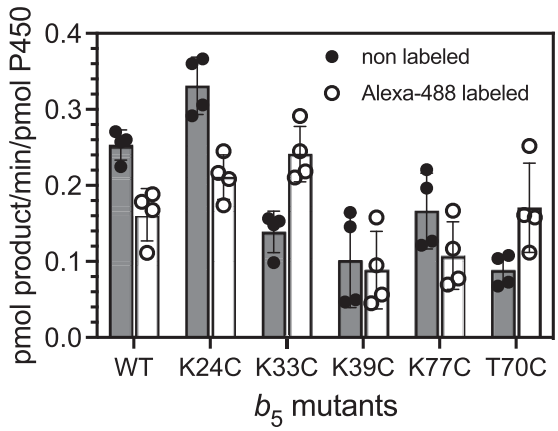

Figure 8. Stimulation of the P450 17A1-catalyzed 17α-OH pregnenolone 17,20-lyase reaction by unlabeled or Alexa 488-labeled WT b_5 and variants. P450 17A1 (25 pmol) was reconstituted with POR (50 pmol) and b_5 (250 pmol) in the presence of 2 μM 17α-OH pregnenolone. The results are represented as means ± SD of quadruplicate samples obtained from two replicate experiments. POR, NADPH-cytochrome P450 reductase.

Discussion

The 17,20-lyase reactions catalyzed by P450 17A1 (Fig. 1) require b_5, and this complex could be an attractive drug target for the treatment of some human diseases, for example, prostate cancer. We recently developed a fluorescence-based binding assay to visualize this protein-protein interaction

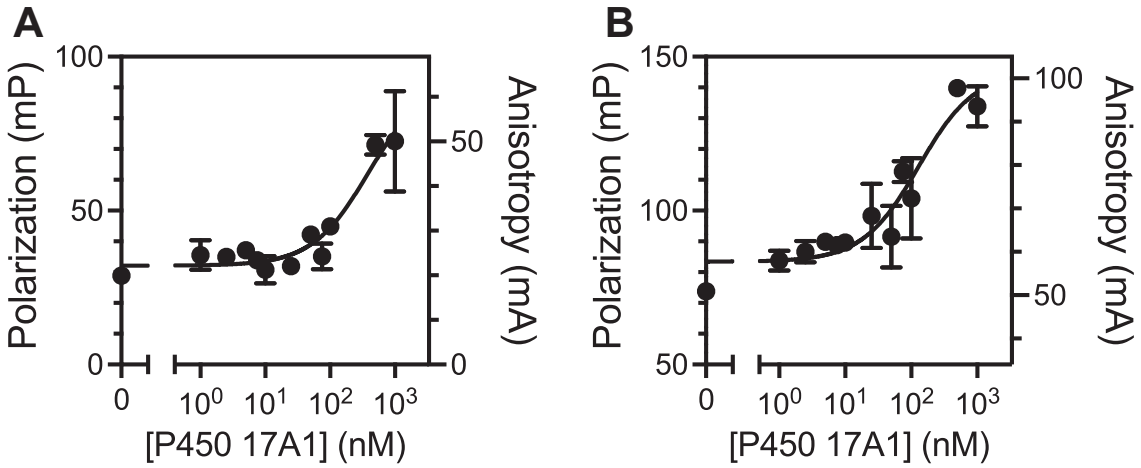

Figure 9. Fluorescence polarization of Alexa 488-labeled T70C and K77C b_5 with P450 17A1. Increasing concentrations of P450 17A1 were added to (*A*) 10 nM Alexa 488-T70C-b_5 or (*B*) Alexa 488-K77C-b_5 in a 384-well plate (final volume 50 μl). Each value represents the mean ± range of duplicate assays. The estimated K_d values were 379 and 125 nM, respectively.

(19). In that report, we utilized site-directed mutagenesis to construct a human b_5 T70C mutant and reacted it with an Alexa 488 fluorophore with a maleimide linker (19). However, we subsequently found that this mutant exists as a dimer and was not tagged with the fluorophore site specifically (Fig. 2). WT b_5 (with no cysteine) could be labeled with the maleimide-containing dye under the same conditions (Fig. 3*A*). The labeled WT b_5 also showed fluorescence quenching when titrated with P450 17A1, as previously observed in the labeled T70C mutant (Fig. 3*B*). Accordingly, we cannot make more conclusions about the details of the site of interaction based on that work (19), in that we were uncertain of the position of the fluorophore (Fig. S5 and Table S2).

Our docking computational model b_5-P450 17A1 structure (Fig. 5) is consistent with some of the interactions identified by chemical cross-linking (32) and by numerous site-directed mutagenesis studies (23, 24, 28, 31). In addition to the interactions reported by Peng *et al.* (32), the model (Fig. 5*A*) also identified five more (Table 2). Functional evidence for the importance of these additional interactions has not been confirmed by site-directed mutagenesis or the observation of clinical variants. Arg-449 was implicated in b_5 interaction by Lee-Robichaud *et al.* (24). The apparent multiplicity of interactions might render further site-directed mutagenesis experiments difficult in light of the multiple contributions of individual residues.

It is known that some heme proteins cause fluorescence quenching when tagged with a green fluorophore, which is suggested to be due to the energy transfer from fluorophores to heme (50, 51). In the case of b_5, an enhanced green fluorescent protein-b_5 fusion protein was constructed, and FRET between enhanced green fluorescent protein and heme was reported (52, 53). We investigated this possibility in our case by utilizing apo-b_5 (Fig. 4), which has previously been shown to be effective in stimulating the lyase activity of P450 17A1 (4, 22). Constructing structurally intact apo-P450 is not known to be possible in the case of the mammalian P450s, to our knowledge. The attenuation of the Alexa 488 dye could also be possible via photoinduced electron transfer by interacting with some amino acids (tryptophan and tyrosine), as presented elsewhere (54, 55). However, the environmental changes around Alexa 488 fluorophore do not solely induce fluorescence quenching, in that emission from Alexa 488-tagged adrenodoxin was shown to increase by binding to P450 27C1, which is also a heme protein (56), although Alexa-adrenodoxin fluorescence was attenuated upon binding to another P450 enzyme, 11A1 (57). In fact, a slight increase was observed in Alexa 488-T70C and Alexa 488-K77C-b_5 when mixed with low concentrations of P450 17A1 (Fig. 7, *E* and *F*), indicating the possible contribution of multiple factors for the observed fluorescence attenuation in our experimental systems.

Cysteine-selective labeling was accomplished by pretreating b_5 variants with 10 mM DTT and limited incubation time (Fig. 6 and Table S2). All of the variants except K19C were shown to bind to P450 17A1 and enhance its lyase activity (Figs. 7, 8, and S6). In one of our previous studies, Alexa 488-T70C b_5 (nonspecifically labeled) did not show any apparent

Table 3
Binding affinities of Alexa-488 labeled mutant b_5 proteins to P450 17A1 or 17A1 peptide estimated from fluorescence polarization measurements (Figs. 9 and 10)

	P450 17A1		P450 17A1 peptide	
Alexa 488-mutatnt b_5	K_d, nM (mean ± SEM)	R^2	K_d, μM (mean ± SEM)	R^2
T70C	379 ± 240	0.815	113 ± 12	0.984
K77C	125 ± 56	0.827	52 ± 9	0.957

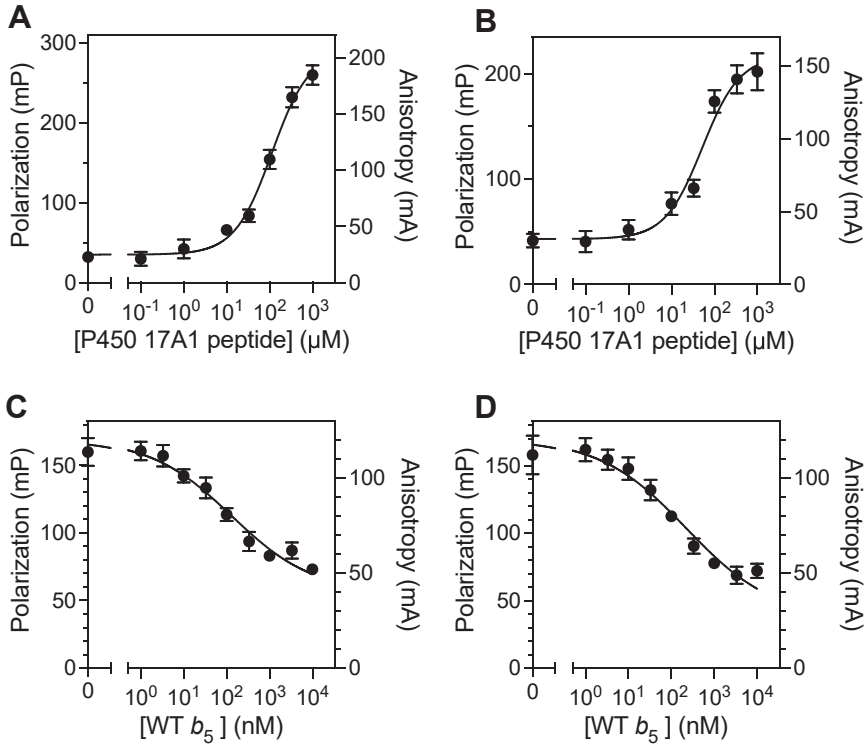

Figure 10. Fluorescence polarization of Alexa 488-labeled T70C and K77C b_5 with P450 17A1 peptide. *A* and *B*, Alexa 488-b_5 T70C (*A*) or K77C (*B*) variants (10 nM) were incubated with various concentrations of the P450 17A1 peptide. Each point represents a mean ± SD of quadruplicate data. The estimated K_d values were 113 μM (T70C, *A*) and 52 μM (K77C, *B*); *C* and *D*, Alexa 488-b_5 T70C (*C*) or K77C (*D*) variants (10 nM) and P450 17A1 peptide (100 μM) complex was incubated with various concentrations of WT b_5 (nonlabeled). Each point represents a mean ± SD of triplicate data. The estimated IC_{50} value of WT b_5 was 129 ± 41 nM (for T70C) and 223 ± 74 nM (for K77C).

binding to P450 2A6 (36) (as reported before on the basis of NMR studies by Bart and Scott (35)) but stimulation of P450 2A6 by b_5 is known (58, 59). Likewise, some inconsistency between binding (of Alexa 488-T70C b_5) and stimulation (by b_5 itself) was observed in the cases of P450s 1A2, 2D6, and 2S1 (36). It may be possible that the presence of the fluorophore prevented labeled b_5 from binding to P450s in these cases, but these examples describe the difficulty of making simple correlations between fluorescence quenching and stimulation of activity. Considering the complexity with the singly labeled Lys-to-Cys b_5 mutants, we did not estimate the binding affinity using the fluorescence attenuation measurements in the present work.

The fluorescence attenuation patterns of the Alexa 488-labeled b_5 mutants are generally consistent with the model we developed (Fig. 5*B*). Lys-24, -39, and –77 and Thr-70 are in positions where the addition of the large fluorophore leads to fluorescence changes upon binding P450 17A1. Lys-19 and Lys-33 are not close (Fig. 5*B*). None of the Lys residues (or Thr-70) appear to be critical in binding of b_5 to P450 17A1, in that the mutants all stimulated 17,20-lyase activity (Fig. 8). The results are consistent with the overall view that the interacting charges on b_5 are all anionic and the charges on P450 17A1 are cationic, although the contribution of other binding forces is possible. The addition of a large fluorophore (Alexa 488) near the binding interface is apparently not enough to eliminate binding, in that stimulation of P450 17A1 17,20-lyase activity was not obliterated.

Another useful fluorescence-based technique to detect protein-protein interactions is fluorescence polarization or fluorescence anisotropy (60). This technology has been used to study protein-protein interactions regarding P450-P450 and P450-POR interactions (61) but to the best to our knowledge, no fluorescence polarization-based assay has been reported for b_5-P450 17A1 interaction. Polarization was observed for b_5 binding to P450 17A1, with K_d values in the range of 100 to 400 nM (Fig. 9 and Table 1). Fluorescence polarization was also applicable to other P450 enzymes, especially P450 3A4 (Fig. S8), known to be one of the most b_5-stimulated hepatic P450 enzymes (58). One interesting finding is that polarization was also observed by adding the P450 17A1 peptide, R_{347}NRLLLLEATIR_{358}, which contains the putative binding site of P450 17A1 including Arg-347 and Arg-358 (Fig. 10, *A* and *B*) (numbering based on the amino acid sequence of P450 17A1). This complex was disrupted by adding (nonlabeled) b_5, showing IC_{50} values of 100 to 200 nM, which are close to the binding affinities of Alexa 488-labeled b_5 variants (Fig. 10, *C* and *D*). Estimated K_d values for the peptide are $\sim 10^3$-fold higher compared with those of the P450 17A1 protein, indicating the weak interaction as observed with its low inhibitory activity against the lyase reaction (19). Besides Arg-347 and Arg-358, Arg-449 and Lys-88 of P450 17A1 are also considered to be critical basic residues for the b_5-P450 17A1 interaction (24, 31, 32). Our model also shows roles of Lys-91, Arg-125, and Arg-126 (Fig. 5*A* and Table 2). The peptide we used lacked these residues, which could be a potential reason

why it showed weak binding. Although interactions with b_5 amino acid residues have not been identified, the P450 17A1 clinical variants P428L, F417C, and E305G are known to have decreased lyase activity (62–64), suggesting the potential importance of these amino acids, which are also lacking in our peptide. Another potential issue is the presence of the Alexa 488 fluorophore which has a net negative charge. This could be more problematic for Alexa 488-labeled peptides because (intramolecular) ionic interactions between the negative charge on the fluorophore and the positive charge on the amino group of arginine in the peptide might prevent the peptide from binding to b_5. Accordingly, further optimization is necessary to develop a peptide-based fluorescence polarization assay.

We have focused on the roles of positively charged P450 17A1 residues and negatively charged residues of b_5 in the interaction of the two proteins (*e.g.*, Fig. 5), and the dependence of binding on ionic strength (Fig. S9) argues for a major effect of this type. However, other interactions may contribute as well. It is of interest that we reported that the (clinically observed) b_5 mutant E305G did not stimulate lyase activity (as already known) or bind well to Alexa-tagged T70C-b_5 in our earlier work (although the site of Alexa labeling was not defined, as we now know). As pointed out earlier, the P450 17A1 clinical variants P428L and F417C show decrease lyase activity as well.

In summary, we have developed several fluorescence-based methodologies to analyze b_5-P450 17A1 protein-protein interactions. Our previously constructed Alexa 488-T70C-b_5 protein contained multiple fluorophores bound at lysines throughout the protein (19), which we have now corrected to have single labeling at sites of mutated cysteines. Other Alexa 488-modified Lys-to-Cys variants were prepared to study the fluorescence quenching but, considering the possible mechanism of this phenomenon, it is still challenging to interpret the active binding and stimulation of lyase activity by only using fluorescence spectra. We report an alternate fluorescence polarization assay utilizing the constructed fluorescently labeled b_5 variants, which provided what is probably a more accurate sub-μM binding affinity to the P450 17A1 protein (Fig. 9 and Table 3). Although the assays with peptides need to be further developed, this approach can provide opportunities to study the b_5-P450 17A1 interaction. Finally, some modern algorithms have recently been developed not only to predict protein structures but also binding interactions. We have used some of these to further refine the current view of b_5:P450 17A1 interactions (Fig. 5, *A* and *B*), including five new putative ionic (or possibly hydrogen) bonding interactions (Table 2).

Experimental procedures

Chemicals and peptides

Alexa Fluor 488 C5 maleimide was purchased from Thermo Fisher Scientific. 17α-OH pregnenolone, dansylhydrazine, and L-α-dilauroyl-*sn*-glycero-3-phosphocholine were purchased from Millipore-Sigma–Aldrich. All other reagents were of analytical grade.

The P450 17A1 peptide (purchased from New England Peptides) was used in our previous report (19). Alexa 488-labeled P450 17A1 peptides were purchased from Thermo Fisher Scientific. The Alexa 488 fluorophore was conjugated to each peptide *via* *N*-hydroxysuccinimide (for N-terminal modification) or maleimide (for C-terminal modification) linker. The sequence of each peptide and the Alexa 488-modified positions are shown below:

P450 17A1 peptide: R_{347}NRLLLLEATIR_{358}

N-terminal modified P450 17A1 peptide: [Alexa 488]-ISDRNR_{347}LLLLEATIR_{358}G

C-terminal modified P450 17A1 peptide: GR_{347}LLLLEA TIR_{358}EVLC-[Alexa 488]

Enzymes

Recombinant rat POR and human P450 17A1 (with a $(His)_6$ tag on the C terminus) were expressed in *Escherichia coli* and purified as described previously (65). The expression plasmids for human b_5 variants were constructed using an Agilent QuikChange II Site-Directed Mutagenesis Kit according to the manufacturer's instructions. Primer pairs for generating each mutant are shown in Table S3. Expression (*E. coli*) and purification procedure of human b_5 variants (45) is described in the Supporting Information. Briefly, b_5 variants were expressed in *E. coli* JM109 cells, the cells were lysed by sonication, and the membrane pellet (which contains b_5) was prepared. After solubilizing the membranes with sodium cholate, the homogenate was centrifuged (10^5 × g), and the resulting supernatant was purified using DEAE anion exchange chromatography. UV-visible spectra of enzymes were recorded using either an OLIS Cary 14 or OLIS DW2a spectrophotometer (On-Line Instrument Systems). Concentrations of P450 17A1 were estimated from Fe^{2+}-CO *versus* Fe^{2+} binding difference spectra using the excitation coefficient $\Delta\varepsilon_{450\text{-}490}$ = 91,000 M^{-1} cm^{-1} (66). The concentrations of b_5 and its variants were calculated using the extinction coefficient ε_{413} = 117,000 M^{-1} cm^{-1} (67) or the difference extinction coefficient $\Delta\varepsilon_{424\text{-}409}$ = 180,000 M^{-1} cm^{-1} for the Fe^{2+} *versus* Fe^{3+} binding difference spectra (68). Apo-b_5 was prepared from human WT b_5 (holo-b_5) by acid-acetone treatment according to a reported procedure (3, 41), and the concentration was estimated by a BCA assay using Pierce BCA Protein Assay Kit (Thermo Fisher Scientific), according to the manufacturer's instructions.

Preparation of Alexa 488-modified b_5 *variants*

Labeling of WT b_5 and apo-b_5 was performed in a similar manner as previously reported (19). WT b_5 (in 100 mM potassium phosphate buffer, pH 7.4) was mixed with Alexa Fluor 488 C5 maleimide (dissolved in dimethyl sulfoxide) at a 1 to 10 molar ratio, then incubated at room temperature overnight in amber glass. Unreacted dye was removed by passage through a Zeba Spin Desalting Column (7K MWCO, Thermo Fisher Scientific) according to the manufacturer's instructions.

For the modification of cysteine-containing b_5 variants, proteins were treated with 10 mM DTT at room temperature for 30 min followed by the above desalting procedure. The reduced proteins were mixed with Alexa Fluor 488 C5 maleimide in a 1 to 5 molar ratio, incubated at room temperature for 2 h, and passed through desalting columns to remove the excess dye. Absorbance spectra of labeled proteins were measured using a Nanodrop spectrophotometer (Thermo Fisher Scientific), and the concentrations of Alexa 488 in the protein sample were calculated using ε_{493} = 72,000 M^{-1} cm^{-1}. The purity of Alexa 488-modified b_5 variants was analyzed by SDS-PAGE.

Proteomic analysis

The in-gel digestion workflow was adapted from the method described by Shevchenko *et al.* (69) with minor changes. Coomassie brilliant blue-stained protein gel bands of interest were excised and diced into ~1 mm^3 cubes. The gel cubes were equilibrated for 5 min in 100 mM NH_4HCO_3 buffer (pH 8.0). Proteins were reduced in-gel with 4.5 mM DTT in 100 mM NH_4HCO_3 buffer (pH 8.0) at 55 °C for 20 min followed by alkylation with 10 mM iodoacetamide in 100 mM NH_4HCO_3 buffer (pH 8.0) at room temperature in the dark for 20 min. Gel pieces were destained with a 1:1 mixture (v/v) of 100% CH_3CN and 50 mM NH_4HCO_3 (pH 8.0), dehydrated by the addition of 100% CH_3CN, and dried in a centrifugal vacuum concentrator prior to proteolytic digestion. Trypsin Gold, mass spectrometry grade (Promega), diluted in 25 mM NH_4HCO_3 buffer (pH 8.0, 10 ng μl^{-1}), was added to cover the dehydrated gel pieces, on ice. After 20 min, an additional 10 µl of 25 mM NH_4HCO_3 buffer (pH 8.0) was added to the gel pieces, and digestion was performed by incubation at 37 °C for 16 h. The resulting tryptic peptides were recovered by two extractions (15 min each) with 50 µl of 60% CH_3CN/0.1% CF_3CO_2H (v/v). The extracts were combined and dried in a centrifugal vacuum concentrator. Peptides were reconstituted in 0.2% HCO_2H (v/v) for analysis by liquid chromatography with tandem mass spectrometry. An analytical column was packed in-house with 20 cm of C_{18} reversed phase packing material (Jupiter, 3 µm beads, 300 Å, Phenomenex) directly into a laser-pulled emitter tip. Peptides were loaded on the capillary reversed phase analytical column (360 µm O.D. × 100 µm I.D.) using a Dionex Ultimate 3000 nanoLC and autosampler. The mobile phase solvents consisted of 0.1% HCO_2H, 99.9% H_2O (solvent A) and 0.1% HCO_2H, and 99.9% CH_3CN (solvent B) (all v/v). Peptides were gradient eluted at a flow rate of 350 nl min^{-1} using an 80 min gradient. The gradient consisted of the following mixtures: 1 to 64 min, 2 to 40% B; 64 to 71 min, 40 to 95% B; 71 to 72 min, 95-2% B; 72 to 80 min (column re-equilibration), 2% B (all v/v). Peptides were analyzed on an Orbitrap Exploris 480 mass spectrometer (Thermo Fisher Scientific), equipped with a nanoelectrospray ionization source. The data-dependent instrument method consisted of MS1 (R = 60000) using an AGC target of 3e6, followed by up to 15 MS/MS scans (R = 15,000) of the most abundant ions detected in the preceding MS scan. The intensity threshold for triggering data-dependent scans was set to 2.0e4, and the MS2 AGC target was 1e5. Dynamic exclusion was enabled with an exclusion duration of 10s, and higher-energy collisional dissociation collision energy was set to 28% nce.

For the identification of peptides, tandem mass spectra were searched with MSFragger (Fragpipe version 19.1, https://msfraggere.nesvilab.org) (70) using the MSFragger default configuration, including the following customizations. Data were searched against a *Homo sapiens* (human) subset database (downloaded 10 May 2021) from the UniprotKB protein database (www.uniprot.org). For analysis of mutant b_5, the human database was appended with the T70C b_5 sequence. Precursor mass tolerance was set to ±20 ppm and fragment mass tolerance to 20 ppm. Enzyme specificity was set to trypsin, and a maximum of two missed cleavages were allowed. Variable modifications included +15.9949 on Met (oxidation), +57.0214 on Cys (carbamidomethylation), +42.01056 on the N terminus (acetylation), +716.1095 on Cys and Lys (Alexa 488 fluorophore), +716.1095 on N-terminus (Alexa 488 fluorophore), +698.0989 on Cys and Lys (Alexa 488 fluorophore), +698.0989 on N terminus (Alexa 488 fluorophore). The target-decoy false discovery rate for peptide and protein identification was set to 1% for both peptides and proteins. Search results were assembled using Scaffold 5.1.2 (Proteome Software, https://www.proteomesoftware.com/products/scaffold-5). Peptide identifications were filtered following manual examination of assigned spectra.

Protein complex modeling with AFM and Rosetta

A structural model of P450 17A1 bound with b_5 was built using the AFM (37) protein structure prediction method, made available through the ColabFold interface (71) (https://colab.research.google.com/github/sokrypton/ColabFold/blob/main/AlphaFold2.ipynb). Because all five models generated by AFM are generally similar to each other (except that the transmembrane helix of b_5 in one model adopts a different pose than the rest of the models, Fig. 11*A*), we selected the model top ranked by AFM for subsequent calculations. We grafted the heme prosthetic group for P450 17A1 from a crystal structure of P450 17A1 (Protein Data Bank ID: 3SWZ) (20) by aligning the crystal structure to the structure predicted by AFM (r.m.sd = 0.71 Å) using PyMOL. The heme prosthetic group for b_5 was similarly grafted from the NMR structure of human b_5 (Protein Data Bank ID: 2I96). The heme-grafted structural model for the b_5-P450 17A1 complex was then subjected to relaxation into the Rosetta energy function (72). The goal of this energy-minimization step was to remove suboptimal geometries in the structure through minor adjustment of the coordinates of atoms causing the suboptimal geometries. Out of the 1000 models generated by the Rosetta FastRelax protocol (73), the lowest-scoring model was selected as the starting pose for further protein-protein docking using Rosetta (38, 74). Before docking, residues 1 to 46 in P450 17A1

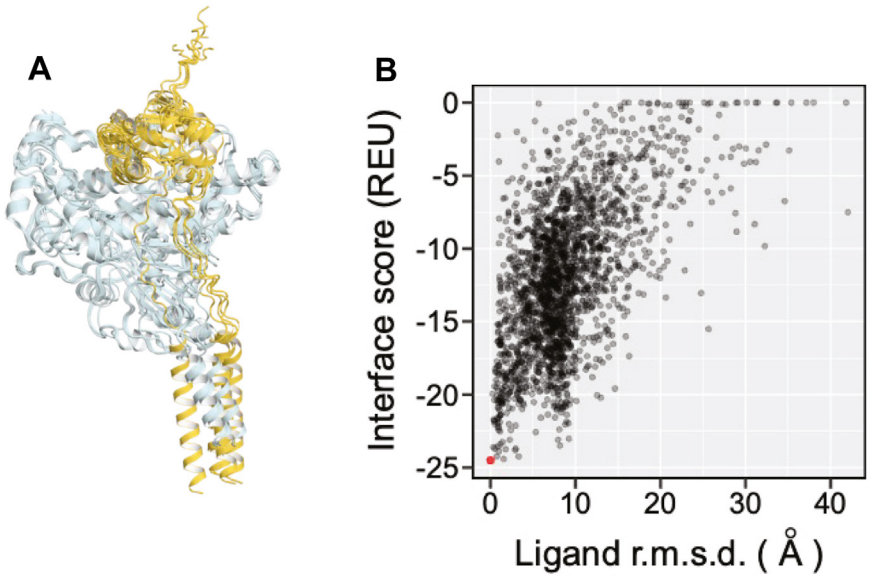

Figure 11. Development of the AlphaFold-Multimer model. *A*, all five models of the b_5-P450 17A1 complex as predicted by AlphaFold-Multimer (overlaid, *cyan*: P450 17A1, *yellow*: b_5). The transmembrane helix of b_5 in one of the models adopts a pose different from those in the other four models. *B*, scatter plot of Rosetta interface score *versus* ligand root-mean-square distance (r.m.s.d.). The *red dot* represents the docked complex with the lowest interface score (in Rosetta Energy Unit, or REU, more negative values indicate stronger binding). This complex was selected for structural analysis. Ligand r.m.s.d. measures the average deviation of ligand (b_5) residues in all other docked models from the ligand residues in the lowest-energy model. The plot is indicative of a typical "energy funnel" where binding becomes stronger (more negative interface score) as r.m.s.d. becomes smaller, suggesting the convergence of docking.

and residues 1 to 8 and 95 to 134 were removed because they are either in the transmembrane helix and its associated loop or the N-terminal loop (residues 1–8 in b_5) and we expect AFM to be less accurate in these regions. In protein-protein docking, we treated b_5 as the ligand and set the values of perturbation flags as -dock_pert 3.8, -dock_mcm_trans_magnitude 0.7, and -dock_mcm_rot_magnitude 5.0. With protein-protein docking, we generated 2000 models of the b_5-P450 17A1 complex with good convergence (Fig. 11*B*) and selected the model with the best interface score for structural analysis in this work. We note that after aligning the docked structure to the AFM-predicted structure based only on P450 17A1 atoms, the backbone r.m.sd for b_5 is 1.1 Å. This result shows good agreement between deep-learning based prediction and biophysical modeling for b_5-P450 17A1 structure.

Titrations with fluorescent b_5

P450 17A1 or hemin (0–180 nM final concentration) was titrated into a solution of Alexa 488-labeled WT b_5 or each of the b_5 variants (50 nM, based on the protein concentration) in 1 mM potassium phosphate buffer (pH 7.4) in a 1.0-cm quartz cuvette (Starna Cells, Inc, catalog # 29F-Q-10). Fluorescence spectra (excitation wavelength 493 nm, emission wavelength 500–600 nm) were recorded using an OLIS DM-45 spectrofluorimeter, with 1.24 mm slits (5.0 nm bandwidth). The data points were normalized to the initial fluorescence intensity at the emission maximum (508 nm). To examine the effect of nonlabeled b_5, WT b_5 (0–200 nM) was titrated into a complex of Alexa-modified b_5 (50 nM) and P450 17A1 (150 nM) in 1 mM potassium phosphate buffer, pH 7.4 (Figs. S3*A*, and S6).

17α-OH pregnenolone lyase reaction catalytic assays

These reactions were performed as previously described, with some modifications (45). Briefly, 0.5 ml reconstituted systems were prepared in 50 mM potassium phosphate buffer (pH 7.4) with P450 17A1 (0.05 μM), 17α-OH pregnenolone (2.0 μM), Alexa 488-labeled or nonlabeled b_5 (0.5 μM), POR (0.5 μM), and L-α-dilauroyl-*sn*-glycero-3-phosphocholine (30 μM). These reactions were preincubated at 37 °C for 5 min before initiation of the reactions by the addition of an NADPH-generating system (0.5 mM $NADP^+$, 10 mM glucose 6-phosphate, and 2 μg ml^{-1} yeast glucose 6-phosphate dehydrogenase (75)). The reactions proceeded at 37 °C for 5 min before being quenched with 2 ml of CH_2Cl_2 and centrifuged at 10^3g for 5 min. The product was derivatized with dansylhydrazine and analyzed by LC-MS according to a reported procedure (16, 45).

Fluorescence polarization assays

Fluorescence polarization assays were performed in a 384-well, black, flat-bottom nonbinding plates (Greiner Bio One, Kremsmünster, Austria/Millipore-Sigma-Aldrich). P450 17A1 protein, P450 17A1 peptide, or WT b_5 were mixed with Alexa 488-labeled proteins or peptides (10 nM) in 1 mM potassium phosphate buffer, pH 7.4 (final volume of 50 μl). After centrifugation at 10^3g for 1 min, each plate was gently shaken for 5 min under the protection from light and read on a Synergy Neo plate reader (BioTek). Blank wells (without

fluorescently labeled material) were included in each experiment and the parallel and perpendicular intensity ($I_{\parallel}$ and $I_{\perp}$, respectively) were subtracted from each data point. Polarization and anisotropy values were calculated using the following equations (76);

$$\text{Polarization (mP)} = (I_{\parallel} - I_{\perp}) \ / \ (I_{\parallel} + I_{\perp}) \times 10^3$$

$$\text{Anisotropy (mA)} = (I_{\parallel} - I_{\perp}) \ / \ (I_{\parallel} + 2I_{\perp}) \times 10^3$$

The anisotropy data points were used for the analysis a quadratic equation in GraphPad Prism software (La Jolla, CA; https://www.graphpad.com/features) to calculate the K_d values using the following equation,

$$Y = \text{A} + \frac{(\text{B}-\text{A})}{2E}\left[(Kd + E + X) - \sqrt{(Kd+E+X)^2 - 4EX}\right]$$

where Y is the observed anisotropy, E is the concentration of Alexa-488 modified b_5 variants, X is the concentration of binding partner, K_d is the dissociation constant, and A and B are the anisotropies of free and bound species, set in Prism as: Y = A+(B-A)*(0.5*(1/E)*((Kd+E+X)-sqrt((Kd+E+X)^2-(4*E*X)))).

Data availability

All data needed to evaluate the conclusions in the manuscript are present in the manuscript and/or the Supporting Information. The mass spectrometry proteomics data have been deposited to the ProteomeXchange Consortium *via* the PRIDE partner repository with the dataset identifier PXD047758.

Supporting information—This article contains supporting information. Detailed experimental procedure for expression and purification of b_5 and P450 17A1 and reduction of b_5 by POR, figures of treatment of T70C b_5 by reducing agents, absorbance spectra of P450 17A1 and hemin, additional flruoescence titrations, tandem mass spectra of modified Lys-containing peptides, SDS-PAGE of purified b_5, reduction of POR-b_5 complex, additional fluorescence polarizaiton assays, and tables of coveragge and list of peptides in proteomic analysis, primer sequences for mutagenesis, and rates of reduction of b_5 by POR (36, 45, 46, 59).

Acknowledgments—Proteomics analyses were supported in part by the Vanderbilt-Ingram Cancer Center grant P30CA068485 (National Institutes of Health). Fluorescence polarization assay experiments were performed in the Vanderbilt High Throughput Screening (HTS) Core Facility with assistance provided by Drs. J. A. Bauer and M. Dehui. The HTS Core receives support from the Vanderbilt Institute of Chemical Biology and the Vanderbilt-Ingram Cancer Center (P30 CA68485).

Author contributions—Y. T., S. N. W., B. L., K. L. R., and F. P. G. methodology; Y. T., S. N. W., B. L., K. L. R., and M. L. formal analysis; Y. T., S. N. W., B. L., L. L., and P. P. investigation; Y. T., B. L., K. L. R., P. P, and F. P. G. writing–original draft; Y. T., B. L., and K. L. R. visualization; Y. T., K. L. R., M. L., and F. P. G. validation; Y. T. and F. P. G. conceptualization; Y. T. and F. P. G. writing–review and editing; Y. T. and F. P. G. supervision; F. P. G. funding acquisition; F. P. G. project administration.

Funding and additional information—This study was supported by the National Institutes of Health grant R01 GM118122 (F. P. G.). The content is solely the responsibility of the authors and does not necessarily represent the official views of the National Institutes of Health. Bian Li contributed to this article as an employee of Vanderbilt University Medical Center and the views expressed do not necessarily represent the views of Regeneron Pharmaceuticals Inc (current employer).

Conflict of interest—The authors declare that they have no conflict of interest with the contents of this article.

Abbreviations—The abbreviations used are: AFM, AlphaFold-multimer; POR, NADPH-cytochrome P450 reductase.

References

1. Noshiro, M., Ullrich, V., and Omura, T. (1981) Cytochrome b_5 as electron donor for oxy-cytochrome P-450. *Eur. J. Biochem.* **116**, 521–526
2. Bhatt, M. R., Khatri, Y., Rodgers, R. J., and Martin, L. L. (2017) Role of cytochrome b_5 in the modulation of the enzymatic activities of cytochrome P450 17α-hydroxylase/17,20-lyase (P450 17A1). *J. Steroid Biochem. Mol. Biol.* **170**, 2–18
3. Yamazaki, H., Johnson, W. W., Ueng, Y.-F., Shimada, T., and Guengerich, F. P. (1996) Lack of electron transfer from cytochrome b_5 in stimulation of catalytic activities of cytochrome P450 3A4. Characterization of a reconstituted cytochrome P450 3A4/NADPH-cytochrome P450 reductase system and studies with apo-cytochrome b_5. *J. Biol. Chem.* **271**, 27438–27444
4. Auchus, R. J., Lee, T. C., and Miller, W. L. (1998) Cytochrome b_5 augments the 17,20-lyase activity of human P450c17 without direct electron transfer. *J. Biol. Chem.* **273**, 3158–3165
5. Yamazaki, H., Shimada, T., Martin, M. V., and Guengerich, F. P. (2001) Stimulation of cytochrome P450 reactions by apo-cytochrome b_5: evidence against transfer of heme from cytochrome P450 3A4 to apo-cytochrome b_5 or heme oxygenase. *J. Biol. Chem.* **276**, 30885–30891
6. Burris-Hiday, S. D., and Scott, E. E. (2021) Steroidogenic cytochrome P450 17A1 structure and function. *Mol. Cell. Endocrinol.* **528**, 111261
7. Vera-Badillo, F. E., Templeton, A. J., de Gouveia, P., Diaz-Padilla, I., Bedard, P. L., Al-Mubarak, M., *et al.* (2014) Androgen receptor expression and outcomes in early breast cancer: a systematic review and meta-analysis. *J. Natl. Cancer Inst.* **106**, djt319
8. Carey, A. H., Waterworth, D., Patel, K., White, D., Little, J., Novelli, P., *et al.* (1994) Polycystic ovaries and premature male pattern baldness are associated with one allele of the steroid metabolism gene CYP17. *Hum. Mol. Genet.* **3**, 1873–1876
9. Gorai, I., Tanaka, K., Inada, M., Morinaga, H., Uchiyama, Y., Kikuchi, R., *et al.* (2003) Estrogen-metabolizing gene polymorphisms, but not estrogen receptor-alpha gene polymorphisms, are associated with the onset of menarche in healthy postmenopausal Japanese women. *J. Clin. Endocrinol. Metab.* **88**, 799–803
10. Valassi, E., Aulinas, A., Glad, C. A., Johannsson, G., Ragnarsson, O., and Webb, S. M. (2017) A polymorphism in the CYP17A1 gene influences the therapeutic response to steroidogenesis inhibitors in Cushing's syndrome. *Clin. Endocrinol. (Oxf.)* **87**, 433–439
11. Chuang, J. Y., Lo, W. L., Ko, C. Y., Chou, S. Y., Chen, R. M., Chang, K. Y., *et al.* (2017) Upregulation of CYP17A1 by Sp1-mediated DNA demethylation confers temozolomide resistance through DHEA-mediated protection in glioma. *Oncogenesis* **6**, e339

12. Bird, I. M., and Abbott, D. H. (2016) The hunt for a selective 17,20 lyase inhibitor; learning lessons from nature. *J. Steroid Biochem. Mol. Biol.* **163**, 136–146
13. Malikova, J., Brixius-Anderko, S., Udhanea, S. S., Parween, S., Dick, B., Bernhardt, R., *et al.* (2017) CYP17A1 inhibitor abiraterone, an anti-prostate cancer drug, also inhibits the 21-hydroxylase activity of CYP21A2. *J. Steroid Biochem. Mol. Biol.* **174**, 192–200
14. Udhane, S. S., Dick, B., Hu, Q., Hartmann, R. W., and Pandey, A. V. (2016) Specificity of anti-prostate cancer CYP17A1 inhibitors on androgen biosynthesis. *Biochem. Biophys. Res. Commun.* **477**, 1005–1010
15. Wróbel, T. M., Jorgensen, F. S., Pandey, A. V., Grudzinska, A., Sharma, K., Yakubu, J., *et al.* (2023) Non-steroidal CYP17A1 inhibitors: discovery and assessment. *J. Med. Chem.* **66**, 6542–6566
16. Guengerich, F. P., McCarty, K. D., Chapman, J. G., and Tateishi, Y. (2021) Stepwise binding of inhibitors to human cytochrome P450 17A1 and rapid kinetics of inhibition of androgen biosynthesis. *J. Biol. Chem.* **297**, 100969
17. Katagiri, M., Kagawa, N., and Waterman, M. R. (1995) The role of cytochrome b_5 in the biosynthesis of androgens by human P450c17. *Arch. Biochem. Biophys.* **317**, 343–347
18. Gonzalez, E., and Guengerich, F. P. (2017) Kinetic processivity of the two-step oxidations of progesterone and pregnenolone to androgens by human cytochrome P450 17A1. *J. Biol. Chem.* **292**, 13168–13185
19. Kim, D., Kim, V., McCarty, K. D., and Guengerich, F. P. (2021) Tight binding of cytochrome b_5 to cytochrome P450 17A1 is a critical feature of stimulation of C21 steroid lyase activity and androgen synthesis. *J. Biol. Chem.* **296**, 100571
20. DeVore, N. M., and Scott, E. E. (2012) Structures of cytochrome P450 17A1 with prostate cancer drugs abiraterone and TOK-001. *Nature* **482**, 116–119
21. Simonov, A. N., Holien, J. K., Yeung, J. C., Nguyen, A. D., Corbin, C. J., Zheng, J., *et al.* (2015) Mechanistic scrutiny identifies a kinetic role for cytochrome b_5 regulation of human cytochrome P450c17 (CYP17A1, P450 17A1). *PLoS One* **10**, e0141252
22. Guengerich, F. P., Wilkey, C. J., Glass, S. M., and Reddish, M. J. (2019) Conformational selection dominates binding of steroids to human cytochrome P450 17A1. *J. Biol. Chem.* **294**, 10028–10041
23. Geller, D. H., Auchus, R. J., and Miller, W. L. (1999) P450c17 mutations R347H and R358Q selectively disrupt 17,20-lyase activity by disrupting interactions with P450 oxidoreductase and cytochrome b_5. *Mol. Endocrinol.* **13**, 167–175
24. Lee-Robichaud, P., Akhtar, M. E., Wright, J. N., Sheikh, Q. I., and Akhtar, M. (2004) The cationic charges on Arg347, Arg358 and Arg449 of human cytochrome P450c17 (CYP17) are essential for the enzyme's cytochrome b_5-dependent acyl-carbon cleavage activities. *J. Steroid Biochem. Mol. Biol.* **92**, 119–130
25. Auchus, R. J. (2017) Steroid 17-hydroxylase and 17,20-lyase deficiencies, genetic and pharmacologic. *J. Steroid Biochem. Mol. Biol.* **165**, 71–78
26. Miller, W. L., Auchus, R. J., and Geller, D. H. (1997) The regulation of 17, 20 lyase activity. *Steroids* **62**, 133–142
27. Gupta, M. K., Geller, D. H., and Auchus, R. J. (2001) Pitfalls in characterizing P450c17 mutations associated with isolated 17,20-lyase deficiency. *J. Clin. Endocrinol. Metab.* **86**, 4416–4423
28. Naffin-Olivos, J. L., and Auchus, R. J. (2006) Human cytochrome b_5 requires residues E48 and E49 to stimulate the 17,20-lyase activity of cytochrome P450c17. *Biochemistry* **45**, 755–762
29. Kok, R. C., Timmerman, M. A., Wolffenbuttel, K. P., Drop, S. L., and de Jong, F. H. (2010) Isolated 17,20-lyase deficiency due to the cytochrome b_5 mutation W27X. *J. Clin. Endocrinol. Metab.* **95**, 994–999
30. Idkowiak, J., Randell, T., Dhir, V., Patel, P., Shackleton, C. H., Taylor, N. F., *et al.* (2012) A missense mutation in the human cytochrome b_5 gene causes 46,XY disorder of sex development due to true isolated 17,20 lyase deficiency. *J. Clin. Endocrinol. Metab.* **97**, E465–E475
31. Estrada, D. F., Laurence, J. S., and Scott, E. E. (2013) Substrate-modulated cytochrome P450 17A1 and cytochrome b_5 interactions revealed by NMR. *J. Biol. Chem.* **288**, 17008–17018
32. Peng, H. M., Liu, J., Forsberg, S. E., Tran, H. T., Anderson, S. M., and Auchus, R. J. (2014) Catalytically relevant electrostatic interactions of cytochrome P450c17 (CYP17A1) and cytochrome b_5. *J. Biol. Chem.* **289**, 33838–33849
33. Ershov, P. V., Yablokov, E. O., Florinskaya, A. V., Mezentsev, Y. V., Kaluzhskiy, L. A., Tumilovich, A. M., *et al.* (2019) SPR-Based study of affinity of cytochrome P450s/redox partners interactions modulated by steroidal substrates. *J. Steroid Biochem. Mol. Biol.* **187**, 124–129
34. Johnson, K. A. (2019). In *Kinetic Analysis for the New Enzymology*, 1st ed., KinTek, Austin, TX: 252–253
35. Bart, A. G., and Scott, E. E. (2017) Structural and functional effects of cytochrome b_5 interactions with human cytochrome P450 enzymes. *J. Biol. Chem.* **292**, 20818–20833
36. Kim, D., Kim, V., Tateishi, Y., and Guengerich, F. P. (2021) Cytochrome b_5 binds tightly to several human cytochrome P450 enzymes. *Drug Metab. Dispos.* **49**, 902–909
37. [preprint] Evans, R., O'Neill, M., Pritzel, A., Antropova, N., Senior, A., Green, T., *et al.* (2022) Protein complex prediction with AlphaFold-Multimer. *bioRxiv*. https://doi.org/10.1101/2021.10.04.463034
38. Leaver-Fay, A., Tyka, M., Lewis, S. M., Lange, O. F., Thompson, J., Jacak, R., *et al.* (2011) ROSETTA3: an object-oriented software suite for the simulation and design of macromolecules. *Methods Enzymol.* **487**, 545–574
39. Albertolle, M. E., Kim, D., Nagy, L. D., Yun, C. H., Pozzi, A., Savas, Ü., *et al.* (2017) Heme-thiolate sulfenylation of human cytochrome P450 4A11 functions as a redox switch for catalytic inhibition. *J. Biol. Chem.* **292**, 11230–11242
40. Stayton, P. S., Fisher, M. T., and Sligar, S. G. (1988) Determination of cytochrome b_5 association reactions: characterization of metmyoglobin and cytochrome P-450$_{cam}$ binding to genetically engineered cytochrome b_5. *J. Biol. Chem.* **263**, 13544–13548
41. Falk, J. E. (1964) *Porphyrins and Metalloporphyrins. Their General, Physical and Coordination Chemistry, and Laboratory Methods*. Elsevier, Amsterdam/New York: 213–230
42. Means, G. E., and Feeney, R. E. (1971) *Chemical Modification of Proteins*. Holden-Day, San Francisco: 66–67
43. Katagiri, M., Suhara, K., Shiroo, M., and Fujimura, Y. (1982) Role of cytochrome b_5 in the cytochrome P-450-mediated C21-steroid 17,20-lyase reaction. *Biochem. Biophys. Res. Commun.* **108**, 379–384
44. Lee, S. G., Kim, V., Lee, G. H., Kim, C., Jeong, E., Guengerich, F. P., *et al.* (2023) Hydroxylation and lyase reactions of steroids catalyzed by mouse cytochrome P450 17A1 (Cyp17a1). *J. Inorg. Biochem.* **240**, 112085
45. Guengerich, F. P., Tateishi, Y., McCarty, K. D., and Liu, L. (2023) Steroid 17α-hydroxylase/17,20-lyase (cytochrome P450 17A1). *Methods Enzymol.* **689**, 39–63
46. Guengerich, F. P. (2005) Reduction of cytochrome b_5 by NADPH-cytochrome P450 reductase. *Arch. Biochem. Biophys.* **440**, 204–211
47. Lee-Robichaud, P., Akhtar, M. E., and Akhtar, M. (1998) Control of androgen biosynthesis in the human through the interaction of Arg^{347} and Arg^{358} of CYP17 with cytochrome b_5. *Biochem. J.* **332**, 293–296
48. Eyring, H. (1935) The activated complex in chemical reactions. *J. Chem. Phys.* **3**, 107–115
49. Lakowicz, J. R. (2006) Energy transfer. In *Principles of Fluorescence Spectroscopy*, 3rd Ed., Springer, New York: 443–475
50. Takeda, S., Kamiya, N., and Nagamune, T. (2003) A novel protein-based heme sensor consisting of green fluorescent protein and apocytochrome b_{562}. *Anal. Biochem.* **317**, 116–119
51. Koga, S., Yoshihara, S., Bando, H., Yamasaki, K., Higashimoto, Y., Noguchi, M., *et al.* (2013) Development of a heme sensor using fluorescently labeled heme oxygenase-1. *Anal. Biochem.* **433**, 2–9
52. Yantsevich, A. V., Gilep, A. A., and Usanov, S. A. (2009) Conformational stability of cytochrome b_5, enhanced green fluorescent protein, and their fusion protein Hmwb_5-EGFP. *Biochemistry (Mosc)* **74**, 518–527
53. Yantsevich, A. V., Harnostai, I. N., Lukashevich, O. P., Gilep, A. A., and Usanov, S. A. (2007) Engineering, expression, purification, and physicochemical characterization of a chimeric protein, full-length cytochrome b_5-green fluorescence protein (HMWb_5-EGFP). *Biochemistry (Mosc)* **72**, 77–83
54. Chen, H., Ahsan, S. S., Santiago-Berrios, M. B., Abruna, H. D., and Webb, W. W. (2010) Mechanisms of quenching of Alexa fluorophores by natural amino acids. *J. Am. Chem. Soc.* **132**, 7244–7245

55. Choi, J., Kim, S., Tachikawa, T., Fujitsuka, M., and Majima, T. (2011) Unfolding dynamics of cytochrome *c* revealed by single-molecule and ensemble-averaged spectroscopy. *Phys. Chem. Chem. Phys.* **13**, 5651–5658
56. Glass, S. M., Webb, S. N., and Guengerich, F. P. (2021) Binding of cytochrome P450 27C1, a retinoid desaturase, to its accessory protein adrenodoxin. *Arch. Biochem. Biophys.* **714**, 109076
57. McCarty, K. D., Liu, L., Tateishi, Y., Wapshott-Stehli, H. L., and Guengerich, F. P. (2023) The multi-step oxidation of cholesterol to pregnenolone by human cytochrome P450 11A1 is highly processive. *J. Biol. Chem.* **300**, 105495
58. Yamazaki, H., Nakamura, M., Komatsu, T., Ohyama, K., Hatanaka, N., Asahi, S., *et al.* (2002) Roles of NADPH-P450 reductase and apo- and holo-cytochrome b_5 on xenobiotic oxidations catalyzed by 12 recombinant human cytochrome P450s expressed in membranes of *Escherichia coli*. *Prot. Exp. Puif.* **24**, 329–337
59. Yun, C.-H., Kim, K. H., Calcutt, M. W., and Guengerich, F. P. (2005) Kinetic analysis of oxidation of coumarins by human cytochrome P450 2A6. *J. Biol. Chem.* **280**, 12279–12291
60. Lakowicz, J. R. (2006) Protein fluorescence. In *Principles of Fluorescence Spectroscopy*, 3rd Ed., Springer, New York: 529–575
61. Lampe, J. N. (2017) Advances in the understanding of protein-protein interactions in drug metabolizing enzymes through the use of biophysical techniques. *Front. Pharmacol.* **8**, 521
62. Sherbet, D. P., Tiosano, D., Kwist, K. M., Hochberg, Z., and Auchus, R. J. (2003) CYP17 mutation E305G causes isolated 17,20-lyase deficiency by selectively altering substrate binding. *J. Biol. Chem.* **278**, 48563–48569
63. Schwab, K. O., Moisan, A. M., Homoki, J., Peter, M., and Simard, J. (2005) 17α-Hydroxylase/17,20-lyase deficiency due to novel compound heterozygote mutations: treatment for tall stature in a female with male pseudohermaphroditism and spontaneous puberty in her affected sister. *J. Pediat. Endocrinol. Metab.* **18**, 403–411
64. Biason-Lauber, A., Kempken, B., Werder, E., Forest, M. G., Einaudi, S., Ranke, M. B., *et al.* (2000) 17α-hydroxylase/17,20-lyase deficiency as a model to study enzymatic activity regulation: role of phosphorylation. *J. Clin. Endocrinol. Metab.* **85**, 1226–1231
65. Hanna, I. H., Teiber, J. F., Kokones, K. L., and Hollenberg, P. F. (1998) Role of the alanine at position 363 of cytochrome P450 2B2 in influencing the NADPH- and hydroperoxide-supported activities. *Arch. Biochem. Biophys.* **350**, 324–332
66. Omura, T., and Sato, R. (1964) The carbon monoxide-binding pigment of liver microsomes. I. Evidence for its hemoprotein nature. *J. Biol. Chem.* **239**, 2370–2378
67. Strittmatter, P., and Velick, S. F. (1956) The isolation and properties of microsomal cytochrome. *J. Biol. Chem.* **221**, 253–264
68. Holmans, P. L., Shet, M. S., Martin-Wixtrom, C. A., Fisher, C. W., and Estabrook, R. W. (1994) The high-level expression in *Escherichia coli* of the membrane-bound form of human and rat cytochrome b_5 and studies on their mechanism of function. *Arch. Biochem. Biophys.* **312**, 554–565
69. Shevchenko, A., Tomas, H., Havlis, J., Olsen, J. V., and Mann, M. (2006) In-gel digestion for mass spectrometric characterization of proteins and proteomes. *Nat. Prot.* **1**, 2856–2860
70. Kong, A. T., Leprevost, F. V., Avtonomov, D. M., Mellacheruvu, D., and Nesvizhskii, A. I. (2017) MSFragger: ultrafast and comprehensive peptide identification in mass spectrometry-based proteomics. *Nat. Methods* **14**, 513–520
71. Mirdita, M., Schütze, K., Moriwaki, Y., Heo, L., Ovchinnikov, S., and Steinegger, M. (2022) ColabFold: making protein folding accessible to all. *Nat. Methods* **19**, 679–682
72. Alford, R. F., Leaver-Fay, A., Jeliazkov, J. R., O'Meara, M. J., DiMaio, F. P., Park, H., *et al.* (2017) The Rosetta all-atom energy function for macromolecular modeling and design. *J. Chem.Theor. Comput.* **13**, 3031–3048
73. Khatib, F., Cooper, S., Tyka, M. D., Xu, K., Makedon, I., Popovic, Z., *et al.* (2011) Algorithm discovery by protein folding game players. *Proc. Natl. Acad. Sci. U. S. A.* **108**, 18949–18953
74. Gray, J. J., Moughon, S., Wang, C., Schueler-Furman, O., Kuhlman, B., Rohl, C. A., *et al.* (2003) Protein-protein docking with simultaneous optimization of rigid-body displacement and side-chain conformations. *J. Mol. Biol.* **331**, 281–299
75. Guengerich, F. P. (2014) Analysis and characterization of enzymes and nucleic acids relevant to toxicology. In: Hayes, A. W., Kruger, C. L., eds. *Hayes' Principles and Methods of Toxicology*, 6th Ed., CRC Press-Taylor & Francis, Boca Raton, FL: 1905–1964
76. Roehrl, M. H. A., Wang, J. Y., and Wagner, G. (2004) A general framework for development and data analysis of competitive high-throughput screens for small-molecule inhibitors of protein–protein interactions by fluorescence polarization. *Biochemistry* **43**, 16056–16066